The Journal of Chemical Physics

What should the density of amorphous solids be?

Cite as: J. Chem. Phys. **151**, 194506 (2019); https://doi.org/10.1063/1.5113733
Submitted: 09 June 2019 . Accepted: 29 October 2019 . Published Online: 20 November 2019

Xiang-Yuan Cui, Simon P. Ringer, Gang Wang, and Z. H. Stachurski

The Journal of Chemical Physics ARTICLE scitation.org/journal/jcp

What should the density of amorphous solids be?

Cite as: J. Chem. Phys. 151, 194506 (2019); doi: 10.1063/1.5113733
Submitted: 9 June 2019 • Accepted: 29 October 2019 •
Published Online: 20 November 2019

Xiang-Yuan Cui,[1] Simon P. Ringer,[1] Gang Wang,[2] and Z. H. Stachurski[3,a)]

AFFILIATIONS

[1]Australian Centre for Microscopy and Microanalysis, and School of Aerospace, Mechanical and Mechatronic Engineering, The University of Sydney, Sydney, NSW 2006, Australia
[2]Materials Microstructures Laboratory, University of Shanghai, Shanghai, China
[3]Research School of Engineering, CECS, Australian National University, ACT 2600, Australia

[a)]zbigniew.stachurski@anu.edu.au

ABSTRACT

A survey of published literature reveals a difference in the density of amorphous and crystalline solids (organic and inorganic) on the order of 10%–15%, whereas for metallic alloys, it is found to be typically less than 5%. Standard geometric models of atomic packing can account for the polymeric and inorganic glasses without requiring changes in interatomic separations (bond lengths). By contrast, the relatively small difference in density between crystalline and glassy metals (and metallic alloys) implies variations in interatomic separations due to merging orbitals giving rise to reduced atomic volumes. To test this hypothesis, quantum density functional theory computations were carried out on ordered and irregular clusters of aluminum. The results point to decreasing interatomic distances with decreasing coordination, from which one can deduce that the geometrical method of random hard sphere packing significantly underestimates the densities of amorphous metallic alloys.

https://doi.org/10.1063/1.5113733

INTRODUCTION

The density of any substance is given by the ratio of its mass divided by volume, $\rho = m/V$. For a given amount of substance, the mass is fixed; however, the volume can vary depending on pressure, temperature, atomic arrangement, and chemical environment. In the following, we consider pressure and temperature as constant and focus our attention on the atomic arrangements and the chemistry of bonding.

As a rule, the density of an amorphous solid is expected to be less than that of its crystalline form, i.e., $\rho_a < \rho_c$. This assertion is based on the relative atomic packing fractions,

$$\rho_a = (pf_a/pf_c) \times \rho_c. \quad (1)$$

Equation (1) is derived from packings of hard spheres. The packing fraction of the crystalline form is calculated from the unit cell and the assumption of hard radius of the atoms. The packing fraction of the amorphous form is taken to be that found for random packing of hard spheres, which is typically on the order of 0.63. For example, the crystalline unit cell of pure aluminum is fcc with an atomic packing fraction, $pf_c = 0.74$. Aluminum density at standard pressure and temperature is 2.70 g/cm^3, based on the atomic radius of 0.143 nm, and a corresponding atomic volume = 0.0166 nm^3/atom. Assuming the hard sphere model for amorphous aluminum and using the same atomic radius, the predicted density of amorphous aluminum should be $\rho_a = (0.63/0.74) \times 2.70 = 2.30$ g/cm^3, a change of approximately −14.5%.

Comparing known densities of solids with crystalline and amorphous forms supports the above expectation, but also reveals a noticeable trend for the different classes of solids, as shown in Table I. In general, the relative variations in density are small for the first class (metallic), but are significantly larger for the next two classes (ionic and covalent), as pointed out recently by Ref. 20. They also make the point that the fractional molar volume difference in glass forming metal alloys is significantly less than the hard sphere of the same radius value.

The concept of representing atoms by spheres has evolved gradually and over a long period of time. By the early 17th century, Joannis Kepler drew a hexagonal close packing of spheres to illustrate a compact solid. The solid sphere model was developed by John Dalton in the early 19th century and formed the basis for

TABLE I. Densities of some crystalline and amorphous solids at standard temperature and pressure. h = Stachurski (2017), unpubl. results. PE = Polyethylene; iso-PP = isotactic polypropylene.

Crystalline solids	Density (g/cm^3)	Amorphous solids	Density (g/cm^3)	Relative change[a] (%)	References
Crystal. Al (fcc)	2.70	Amor. Al	2.52—2.55	—5.61	h
Crystal. Cu (fcc)	8.96	Amor. Cu	8.48	—5.3	7
Crystal. Si (dc)	2.329	Amorph. Si	2.294	—1.5	61
Crystal. $Zr_{37}Cu_{63}$	7.80	Amor. $Zr_{37}Cu_{63}$	7.68	—1.54	37
Crystal. $Zr_{50}Cu_{50}$	7.40	Amor. $Zr_{50}Cu_{50}$	7.30	—1.41	37
Crystal. Ni_3Nb	8.95	Amor. $Ni_{62}Nb_{38}$	8.72	—1.40	6,23
Cristobalite	2.55	Silica glass	2.20	—13.7	67
α-alumina	3.95	Amor. Al_2O_3 (h.d.)	3.30	—16.4	27
Corundum	4.02	Amor. Al_2O_3 (h.d.)	3.30	—19.9	50
Crystal. As_2Se_3	5.10	Glassy As_2Se_3	4.62	—9.42	67
Crystal. InSb	5.78	Glassy InSb	6.10	+5.54	32
Crystal. PE	1.00	Amor. PE	0.86	—14.4	25
Crystal. iso-PP	0.95	Amor. iso-PP	0.86	—9.61	47
Crystal. Nylon 66	1.22	Amor. Nylon 66	1.07	—12.3	55

[a]Relative change in density: $\Delta\rho = (\rho_a - \rho_c)/\rho_c$.

representations of the structure of crystalline solids and for calculations of packing density. In the 20th century, with the identification of the amorphous structure of solids, one of the earliest analyses of the density of noncrystalline solids was published by Cargill,[11] who compared the random arrangements of hard close packed spheres with those of the amorphous Ni-P alloys. His analysis showed that the atomic arrangements in noncrystalline Ni-P alloys should differ only slightly from those in a dense random packing of spheres, and the small difference observed between packing densities of Ni-P and the corresponding hard sphere model was ~5%. A broader view of the structural differences in atomic arrangements was described in Ref. 54.

Historically, despite its popularity, the simplified hard sphere model had difficulty to account for some seemingly counterintuitive observations in both crystalline and amorphous systems. For example, in Al-Li alloys, increasing Li concentration increases the elastic modulus even though the Young's modulus of Li (14 GPa) is much smaller than that of Al (91 GPa).[43] Recently, by performing accurate density functional theory (DFT) simulation, Alam and Johnson achieved results in fine agreement with experiments in terms of structural properties as well as energetics.[1] Another example concerns Cr-doped GaN. Experimentally, adding a larger Cr substitutional dopant systematically decreases the lattice constants.[51] DFT simulations show this to be due to the formation of embedded Cr clusters with the Cr-Cr distances contracted by up to 17%.[16] A general interpretation of these successes lies in the many-body quantum effects which can be described satisfactorily by density functional theory (DFT) in terms of both the atomic structure as well as the electronic structure,[15] but it was totally overlooked in the hard sphere model. Such effects are particularly significant for systems involving mixed valency and site preference.[2,3] Below, we will show that it is also important in amorphous elemental systems such as Al.

The atomic arrangements in metallic and metalloid solids have long been the subject of numerous investigations, for example, Refs. 13, 21, 26, 40, 46, and 59. In general, the small density differences between the metallic glasses and crystalline solids are accredited to the assertion that a degree of short-range order (SRO) and medium-range order (MRO) exist in the amorphous solid, which increases the overall physical density of the amorphous solid toward that of the crystalline solid. This will be referred to as the SRO/MRO hypothesis.

By contrast, the explanation proposed in this paper is based on the conjecture that the atomic arrangement is essentially random but the consequent reduction in atomic coordination, resulting from random packing, leads to reduced interatomic separations (RIS), thus allowing for higher overall density. This will be referred to as the RIS hypothesis.

Physical reasons and evidence are presented herein to show that the SRO/MRO hypothesis is erroneous. The RIS hypotheses are tested by means of the first principles density functional theory (DFT) method, by computations on pure aluminum clusters of varying coordination in the first shell. Compared to predictions from Eq. (1), the DFT results show that the interatomic spacing decreases with the reduced coordination number around the central atom, thus leading to a reduced atomic volume (increased packing fraction), hence an increased density toward that of the corresponding crystalline form.

DFT COMPUTATIONS

Amorphous aluminum clusters

At present, no physical sample of pure amorphous aluminum has been prepared in a sufficient quantity to determine the physical density by a direct method. Instead, computer simulated clusters

of randomly packed aluminum atoms have been subjected to DFT computations and analysis in order to test the RIS hypothesis. To this end, we performed all-electron DFT calculations on clusters of aluminum using the generalized gradient approximation (GGA)[45] with the DMol^3 program package.[18,19] The wave functions were expanded in terms of a double-numerical quality basis set, with an atomic real-space cut-off equal to 12.75 bohrs for Al.

It is conjectured that rearranging the atomic packing from crystalline to amorphous should result in a change in atomic volumes in clusters of pure aluminum. For this purpose, a large random packing of aluminum atoms (>10^6) was created by the the ideal amorphous solid (IAS) method described elsewhere.[59] In this packing of hard spheres, the distance between nearest neighbors was set to 0.2860 nm, the closest separation between two aluminum atoms in

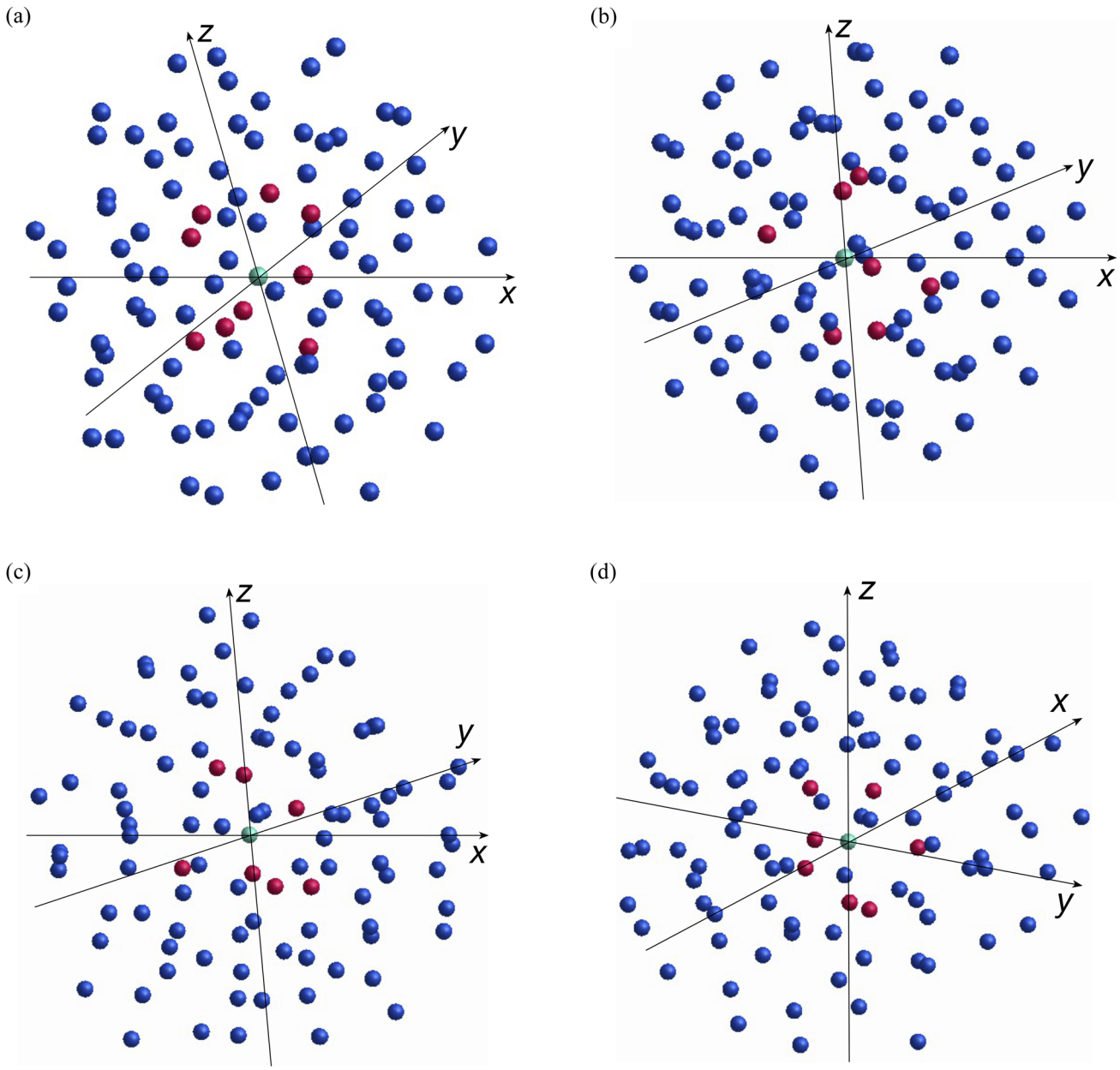

FIG. 1. The studied random clusters of pure aluminum, each comprising 101 atoms extracted from a large IAS amorphous packing. In each cluster, the central atom is colored green and the first shell atoms are colored red: (a) 9 atoms in the first shell and [(b), (c), and (d)] 7 atoms in the first shell. The red atoms are randomly positioned around the central atom, but initially, all are at a fixed distance of 0.2860 nm from the center.

TABLE II. DFT calculated initial (unrelaxed) and relaxed distances, atomic volume, and Mulliken charge of the central atom for the randomly selected clusters (a)–(d), as shown in Fig. 1.

Cluster	Atom coord.	Initial dist. (nm)	Initial vol. (nm^3/at.)	Initial Mull.charge (e)	Relaxed bond dist. (nm)	Relaxed vol. (nm^3/at.)	Relaxed Mull.
(a)	9	0.2860	0.017 014	−0.029	0.2722, 0.2790 0.2810, 0.2837 0.2838, 0.2851 0.2881, 0.2901 0.3154	0.016 653	−0.071
(b)	7	0.2860	0.017 854	−0.016	0.2776, 0.2799 0.2814, 0.2819 0.2830, 0.2854 0.2929	0.017 276	−0.034
(c)	7	0.2860	0.017 567	0.001	0.2795, 0.2803 0.2811, 0.2841 0.2854, 0.2861 0.2909	0.017 065	−0.004
(d)	7	0.2860	0.017 458	−0.078	0.2616, 0.2655 0.2728, 0.2771 0.274, 0.2796 0.2846	0.016 886	−0.219

the fcc lattice. The bulk packing fraction of this model amorphous solid was 0.63 ± 0.005.

Next, several clusters containing 101 atoms have been extracted from the amorphous packing, with a chosen atom as the center of the cluster, and surrounded by the other 100 aluminum atoms at random positions. Convergence tests reveal that the estimated error of the calculated central bond lengths is ~0.001 nm; depending on the cluster, each central atom has different configurations of surrounding atoms, as shown in Fig. 1.

Due to the nonsymmetrical nature of amorphous packing, relaxation during DFT computations leads to the initial first nearest neighbor bonds, initially of the same length, to be no longer equal (Table II column 6). Focusing on the local structures (central part of the clusters), most bond lengths are shortened, but some are elongated. Significantly, the DFT results demonstrate that the interstitial space values are all decreased after considering the quantum interatomic interaction. Such a volume shrinkage is inhomogeneous, depending on the surrounding environment. Collectively, the DFT results demonstrate that quantum effects result in a higher mass density than that of the amorphous aluminum system modeled on packing of hard spheres.

Crystalline aluminum clusters

To corroborate the main results for the amorphous clusters, we have carried out DFT computations on fcc, bcc, and simple

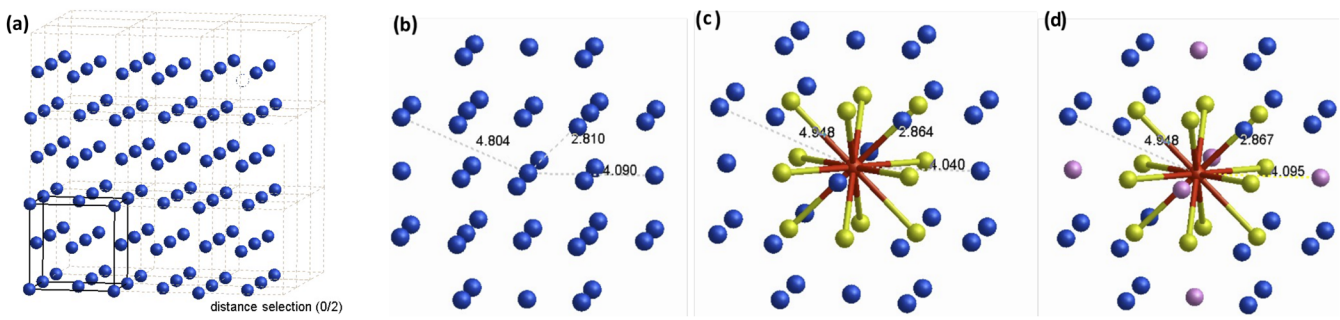

FIG. 2. (a) Fragment of fcc crystalline aluminum, (b) interatomic distances from the central atom, (c) the central aluminum atom (red), 2nd shell 12 (yellow) atoms, and (d) 3rd shell 6 (pink) atoms, 4th shell 24 (blue) atoms.

TABLE III. Calculated data for bulk crystalline Al by the DFT-GGA method.

System	Coord. Number	Bond dist. (nm)	Volume/atom (nm^3/atom)	Density (g/cm^3)	Cohes. energy (eV/atom)	Mulliken Charge
Al-fcc	12	0.2862	0.016 552	2.707	3.342	0
Al-bcc	8	0.2802	0.016 012	2.649	3.246	0
Al-cubic	6	0.2722	0.020 149	2.224	2.971	0

TABLE IV. Results of DFT computations on three ordered clusters shown in Fig. 2.

case	system	1st d_{NN} (nm)	2nd d_{NN} (nm)	3rd d_{NN} (nm)
Reference	Bulk fcc	0.2857	0.4040	0.4948
(i)	Fully relaxed cluster	0.2810	0.4090	0.4804
(ii)	Fix 2nd and 3rd cluster	0.2864	0.4040	0.4948
(iii)	Fix 3rd cluster	0.2867	0.4095	0.4948

cubic clusters of aluminum atoms, with the expectation that even in ordered structures, interatomic spacings will decrease if the first-shell coordination is reduced, as it is in the sequence: fcc → bcc → sc. Schematic drawings of the fcc clusters are shown in Fig. 2. The calculated lattice constant from DFT computations is 0.4040 nm, compared with the experimental value of 0.4049 nm.[66] The computed first nearest neighbor distance (d_{NN}) is 0.2857 nm, the second is 0.4040 nm, and the third is 0.4948 nm (Table III), in good agreement with experimental values, namely, 0.2863 nm, 0.4049 nm, and 0.4961 nm, respectively. The DFT results in Table IV (the Appendix) clearly show that the first nearest neighbor distances decrease with decreasing shell coordination number, thus supporting the observations on the random clusters.

DISCUSSION

Densities of metallic and metalloid solids

Aluminum

Using volume-temperature data from a number of sources,[5,31,36] one can predict the likely density of amorphous aluminum as 2.52–2.55 × 10^3 kg/m^3, as given in Table I. The relative density reduction of around −5.6% is in stark contrast with the value of −14.5% predicted by Eq. (1). A similar result will be found for other pure fcc metals, for example, for pure copper, the change is ∼−4.5%.[8]

Computations of the quantum interatomic interactions in all of the random clusters used here lead to local volumetric shrinkage, although in principle one cannot exclude the possibility of volumetric expansion. Geometric relaxation further enhances the electron charge inhomogeneity. Thus, DFT calculations clearly show that quantum interatomic interactions are important in accounting for the significant deviation of mass density between the simple hard sphere packing model and the DFT derived model. It is also interesting to observe that due to the asymmetry of atomic positions, the atomic Milliken charge values are not zero (as found in the crystalline Al).

Douglass *et al.*[20] found that the effective atomic radii in the amorphous state become increasingly smaller than those in the crystal as the softness of the particles increases, expressed in terms of Morse potential.

$Zr_{50}Cu_{50}$ alloy

Now, consider the $Zr_{50}Cu_{50}$ alloy. As a crystalline solid, this alloy has two martensitic monoclinic structures: one with a measured density of 7.39 g/cm^3 and the other 7.40 g/cm^3, and unit cell volumes, 69.3 $Å^3$ and 69.5 $Å^3$, respectively.[68] It comprises 2 (Zr-Cu) atomic pairs per unit cell. Taking r_{Zr} = 0.155 nm and r_{Cu} = 0.125 nm, the estimated volume packing fraction is ∼0.71. Using Eq. (1) with the appropriate radii for Zr and Cu atoms and the amorphous packing density of pf_a = 0.63, the predicted density of the amorphous alloy is 6.59 g/cm^3, a relative change of approximately −11%. However, the measured density of this amorphous alloy has been reported as 7.30 g/cm^3 by Ref. 37, a relative change close to −1.4%, in large contrast to the above value.

The amorphous nature of the $Zr_{50}Cu_{50}$ alloy has been observed to conform to the expected x-ray scattering pattern for glassy metals.[35] This implies random packing of atoms and consequent topology; for random packing of atoms of two different sizes, the volume fraction varies from the value of 0.63, but not much, as shown in Ref. 44, and the final conclusion is the same. The geometrical method of random hard sphere packing fails to predict the high density of this amorphous metallic alloy relative to its crystalline form. It is conjectured that the quantum interatomic interactions in this alloy also play a role in reducing interatomic spacings, making the alloy more dense than that predicted by the geometrical method.

Similar arguments apply to other alloys of this system[62] for which there are experimental data that confirm the variation in density of between −1% and −3%, as shown in Fig. 3(b). This is also true for many other metallic alloys, as reported by Refs. 30 and 65.

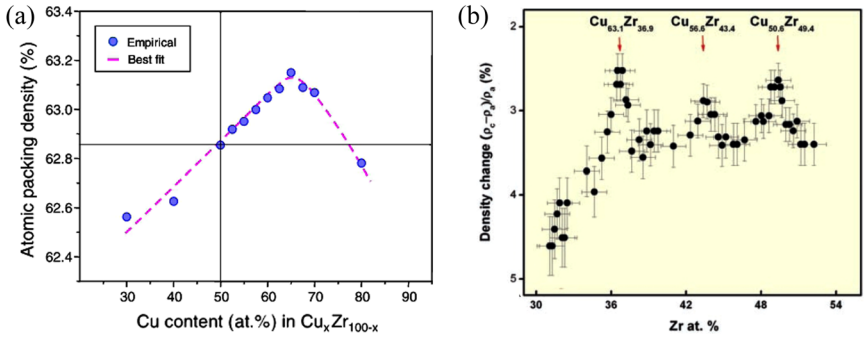

FIG. 3. (a) A small variation of atomic packing with a wide range of composition for the Cu-Zr amorphous alloy. Reproduced with permission from Park *et al.*, Scr. Mater. **57**, 805 (2007). Copyright 2007 Elsevier. (b) Measured relative densities of amorphous and crystalline CuZr alloys. Reproduced with permission from Li *et al.*, Science **322**, 1816 (2008). Copyright 2008 American Association for the Advancement of Science.

Ni_3Nb alloy

The Ni-Nb alloy system has two intermetallic compounds: β-phase (Nb_7Ni_6) and γ-phase (Ni_3Nb), with densities 8.74 g/cm^3[42] and 8.463 g/cm^3,[23] respectively. An alloy of the bulk composition $Ni_{62}Nb_{38}$ would have a density of 8.60 g/cm^3 (calculated by the phase lever rule). The measured density of an amorphous alloy of the same composition is 8.72 g/cm^3,[6] giving a relative change in density of −1.40%, as shown in Table I.

The crystal structure of the γ-phase is orthorhombic (space group Pmmn), with unit cell dimensions taken as: a = 0.5125 nm, b = 0.4261 nm, and c = 0.4538 nm, containing 6 Ni and 2 Nb atoms.[10] The crystal structure is not closed packed, but rather forming two similar (hollow) clusters of atoms, one of which is delineated in Fig. 4(a). The estimated volume packing fraction for this structure is 0.69, with assumed radii r_{Ni} = 0.124 nm and r_{Nb} = 0.130 nm. The electronic structure of this alloy is dominated by the hybridization between the Ni d3 orbital and the Nb d3 orbital, giving the strong negative values of the formation enthalpy. The β-phase is a complex intermetallic compound whose characteristic features are high values of coordination numbers (CN) and mixed occupancy of sublattices by the Nb- and Ni-atoms with the lack of a definite stoichiometry. It is a rhombohedral structure with 13 atoms distributed over 5 lattice sites with CN ranging from 12 to 16.[14] The estimated volume packing fraction is ~0.74.

For the amorphous alloy, $Ni_{62}Nb_{38}$, one should expect a randomly packed atomic structure as evidenced by the shape of the x-ray and neutron scattering structure factors [Fig. 4(c)]. Thus, taking its packing fraction as ~0.63, the theoretical amorphous density of this alloy is predicted by the geometrical packing ratio method as

$$\rho_{a.alloy} = \left(\frac{pf_a}{pf_c}\right)_\beta (vf \times \rho)_\beta + \left(\frac{pf_a}{pf_c}\right)_\gamma (vf \times \rho)_\gamma \quad (2)$$

$$= (0.63/0.74)(0.59 \times 8.74) + (0.63/0.69)(0.41 \times 8.46) = 7.34\ \text{g/cm}^3, \quad (3)$$

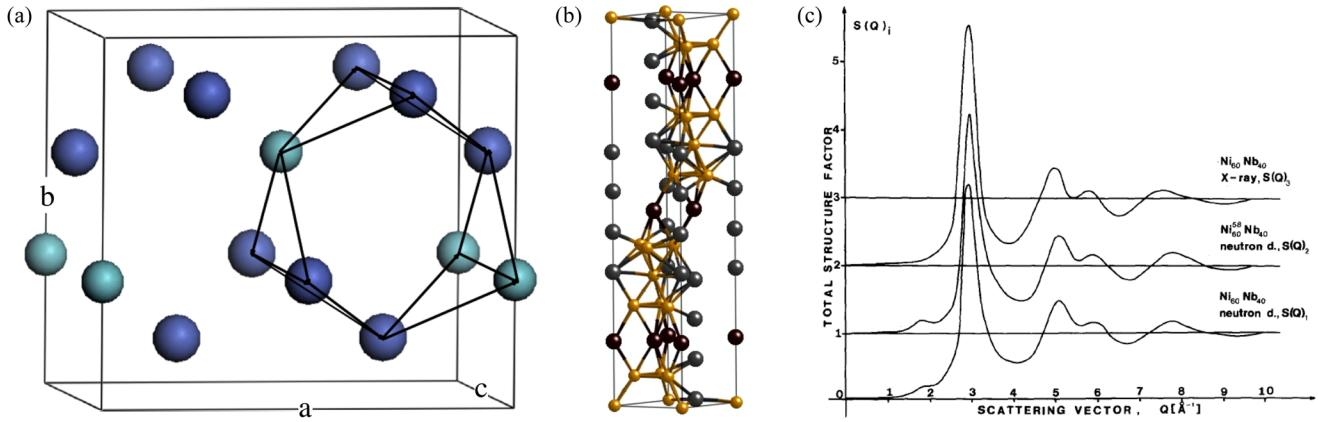

FIG. 4. (a) An orthorhombic crystal unit cell of the Ni_3Nb compound with 6 Ni and 2 Nb atoms per cell: Ni—blue, Nb—green. One hollow cluster outlined by line segments. Adapted with permission from Cao *et al.*, Comput. Mater. Sci. **77**, 208 (2013). Copyright 2013 Elsevier. (b) Crystal unit cell of the Nb_6Ni_7 compound with Ni—gray, Nb—gold. Adapted with permission from P. Nash and A. Nash Bull. Alloy Phase Diagrams **7**, 124 (2013). Copyright 2013 Elsevier. (c) X-ray and neutron static structure factor for Ni-Nb amorphous alloys showing a broad scattering peak characteristic of amorphous structures with random packing of atoms. Reproduced with permission from Svab *et al.*, J. Non-Cryst. Solids **46**, 125 (1981). Copyright 1981 Elsevier.

much lower than that reported by Ref. 6. In Eq. (3), vf means volume fraction. Interestingly, a density of 7.70 g/cm^3 was reported by Ref. 17 for a hard sphere computer simulated alloy of the $Ni_{71}Nb_{29}$ alloy, which is close to the composition and density predicted by Eq. (3). In any case, the difference cannot be reconciled simply by the geometrical method.

Svab *et al.*[57] deduced from x-ray and neutron scattering studies of the amorphous $Ni_{60}Nb_{40}$ alloy that the coordination numbers were 11.8 around the Ni atom and 12.2 around the Nb atom. These numbers were calculated from the areas of the partial scattering peaks and therefore give the average coordination around atoms represented as soft spheres, which would be similar to Voronoi calculations of computer simulated structures using the radical tessellation method of Ref. 4 In such studies, the average coordination number is typically 14–16, indicating perhaps a lower density packing.

A major source of uncertainty in these calculations is the selected size of atoms. Nevertheless, one must observe that the geometrical method, based on packing hard sphere models of atoms, cannot account for the relatively small difference in densities between the crystalline and glassy forms of this metallic alloy. Indeed, it is concluded that electron density changes associated with random packing are responsible for the altered interatomic distances.

Polymeric solids

The so-called saturated polymers, characterized by covalent bonding within the chain structure with no chemical functionality in side groups, and van der Waals bonding between the chains are good examples for applying hard sphere models to packing and for conforming to the general rule on densities based on packing of hard spheres.

For polymethylene, a -[CH2]- monomeric unit can be approximated as a sphere (Fig. 5). Thus, a possible simplified model for an ideal amorphous polymeric solid is as follows: Consider N randomly packed equal sized spheres, each sphere representing the monomer (where N is a large number). Make a chain of touching spheres: chose one sphere as the starting point and thread it with one of its touching neighbors. Next, thread the second sphere at random with one of its touching neighbors, except the one already joined to. Continue in this manner along the three dimensional self-avoiding random walk (SARW) until a chain of $n-1$ links is formed. Next, choose another (unattached) starting sphere and, following the above process, construct another chain of n spheres. Repeat the process until (N/n) chains are formed. Since $N \gg n$, there are many ways to form the chains, and therefore, there exists a finite probability that it is possible to form (N/n) chains without violating the self-avoiding random walk and without any free sphere(s) left over. This structure of linear freely joined chains constitutes an ideal polymeric amorphous solid.[53] According to this model, the packing fraction should be $pf_a = 0.63 \pm 0.01$. Given the density of perfectly crystalline polyethylene[52] as $\rho_c = 1.00$ g/cm^3, the perfectly amorphous polyethylene should have a density of $\rho_a = 1.00 \times (0.63/0.74) = 0.85$ g/cm^3, a change of ~−15%. The experimental value of density is 0.87 g/cm^3, measured on a sequence of semicrystalline polyethylenes with diminishing crystallinity; therefore, a good agreement is obtained.

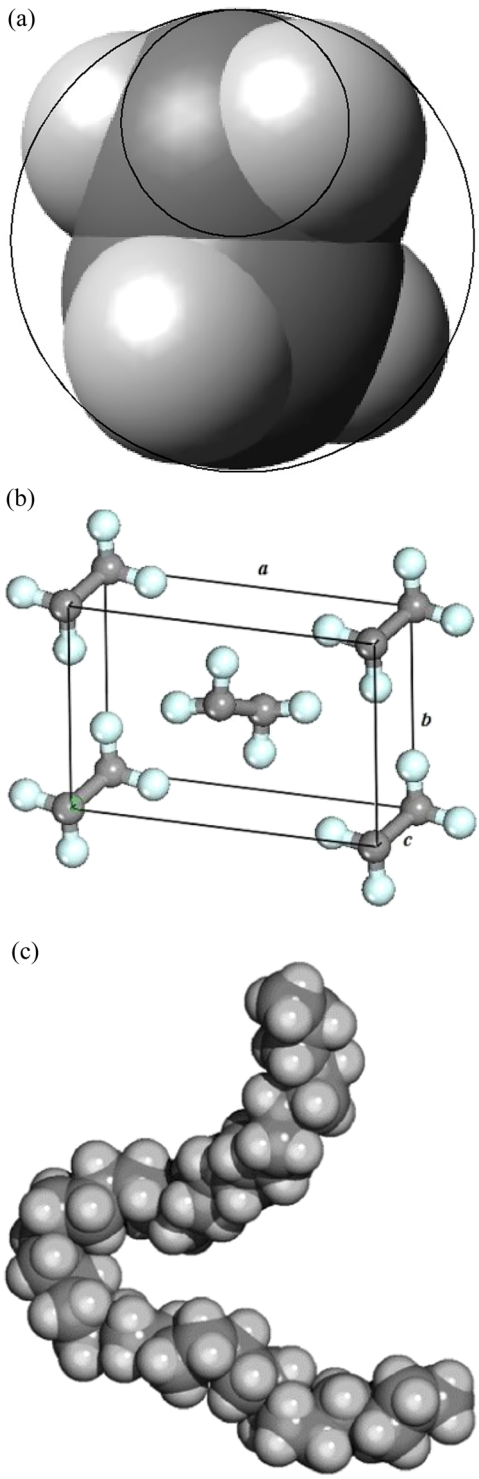

FIG. 5. (a) A C2H4 monomer can be approximated by a sphere, (b) unit cell of crystalline polyethylene, and (c) a fragment of the polyethylene chain with atomic sizes corresponding to realistic atomic dimensions. Reproduced with permission from Muller *et al.*, J. Chem. Phys. **114**, 9764 (2001). Copy right 2001 AIP Publishing LLC.

The above model of touching sphere chains was corroborated by a separate study of chains based on jointed spheres by Ref. 34, who have shown that the hard sphere chains reach their maximally jammed state at the same volume fraction as the packing of single spheres, i.e., 0.638 ± 0.004, regardless of the chain length.

Surprisingly, a study of polymeric chains based on connected spheres by Ref. 69 has found that the packing density reduces to as low as ~0.4 with increasing length of polymer chains, which would give amorphous density of polyethylene as 0.54 g/cm^3, an unrealistically low value. They have taken into account constraints on bond flexing, and the effect of chain ends, and concluded that long linear chains should pack less densely than short linear chains. Their model can be understood as the jamming of semirigid chains when compacted, and it suggests that the molecular geometry can influence the structure of condensed matter.

The unit cell of crystalline polyethylene is orthorhombic with dimensions $a = 0.733$, $b = 0.493$, and $c = 0.256$ nm and contains 4 [CH2] monomers. The carbon atoms along the chain can be represented as interpenetrating spheres of the (van der Waals) radius, $r_C = 0.170$ nm with a C–C distance of 0.154 nm and a C–C–C bond angle, $\alpha = 114°$ in a planar zig-zag configuration. Taking the H-atom's van der Waals radius as $r_H = 0.117$ nm and the interpenetrated distance H–C as 0.109 nm, one can calculate the occupied volume fraction as $pf = 0.72$. On this basis, the predicted density of amorphous polyethylene should be $(0.63/0.72) \times 1.00 = 0.875$ g/cm^3.

Accurate atomistic computer modeling of polymers was pioneered by Theodorou and Suter. A recent realistic model to represent the amorphous structure of polymers has been proposed by Ref. 41, based on computer simulated atomistic models of single polymer chains with the experimentally derived rotational isomeric state. In their model, atoms are represented by overlapping hard spheres of C-atoms and H-atoms to appropriate interatomic distances of covalent bonding, with a corresponding distribution of C–C bond torsional angles. Their result for amorphous polyethylene density is 0.892 g/cm^3. For comparison, one should take the measured density of highly crystalline (extended chain) polyethylene as 1.00 g/cm^3, and using this value calculate the reduction in density as $(0.892/1.00) - 1 = -1.08$ or ~−11%, a value close to that found in Table I.

Analysis of other polymers which have both amorphous and crystalline forms confirms the general trend of −10% to 15% relative difference in their densities. Therefore, one can conclude that the atomistic models for polymers as proposed by Ref. 41 are a good representation of the packing arrangements in organic (saturated bond) polymers. Consequently, the law of simple mixtures, expressing the proportionality of density to crystalline volume fraction, is well proven for semicrystalline polymers. There is no need to invoke the SRO/MRO hypothesis, or the RIS hypothesis.

Ionic solids

For many compounds, the model of ions as hard spheres does not reproduce the distance between ions, d_{mx} to the accuracy with which it can be measured in crystals. One can improve the model by representing ions as "soft spheres" that overlap in the crystal. Because the ions overlap, their separation in the crystal will be less than the sum of their soft-sphere radii.[33]

The concept of ionic radii is based on the assumption of a spherical ion shape. However, from a group-theoretical point of view, the assumption is only justified for ions that reside on high-symmetry crystal lattice sites; chalcogen ions have to be modeled by ellipsoidal charge distributions with different radii along the symmetry axis and perpendicular to it.

The chalcogenide glasses present a more complex problem of predicting atomic arrangements and interatomic distances. This was pointed out in a previous publication.[24]

SRO/MRO hypothesis in metallic alloys

This hypothesis assumes that nanoclusters and microclusters of ordered atomic arrangements are present in amorphous metallic alloys, and that their presence increases the density toward the crystalline value. This implies the law of mixtures (based on the Lewis law for additivity of volumes): $\rho_{alloy} = v_a\rho_a + v_c\rho_c$, where v_a and v_c represent the volume fractions of the amorphous and crystalline phase volume fractions, respectively.

Experimental evidence in favor of the hypothesis is: (i) SRO and MRO usually develop as the quenched bulk metallic glasses (BMG) are annealed;[63,64] the published literature in the presence of the SRO and MRO in bulk metallic glasses is extensive, exemplified by Refs. 9, 28, 38, 39, 49, 56, and 63, (ii) presence of the first sharp diffraction peak is an indication of the MRO,[13,22,48] and (iii) the existence of frozen-in stresses.[60]

The evidence against this hypothesis is that substantial volume fractions of the ordered regions are required to increase the density close to the experimentally observed values, at which point the solid is no longer an amorphous glass but rather a semicrystalline solid. For example, if the ideal amorphous density of $Zr_{37}Cu_{63}$ is $7.80 \times (0.63/0.74) \sim 6.64$ g/cm^3, then the required volume fraction of fcc type clusters to raise the density of the amorphous alloy from 6.64 g/cm^3 to 7.68 g/cm^3 is $v_c \sim 0.9$, i.e., ~90%, as noted above. Similar results are found for the other metallic glasses. Also, if regions of the SRO and MRO of significant extent exist, then the corresponding Braggs' XRD peaks should be observed. Experimentally, no sharp diffraction peaks are observed in metallic glasses [Fig. 6(a)] until they are annealed and reach a significant volume fraction of the ordered clusters, as shown in Fig. 6(b).

The RIS hypothesis for metallic alloys

The variation of interatomic distances under the influence of a given neighborhood chemistry has been observed and quantified by Ref. 12 for a Zr-Cu system with small Al additions. They deduced changes in the interatomic spacing between 3.5% and 2% on addition of 8–15 at. % Al, derived from measurements of elastic constants. One can infer from these results that the solute Al atoms in the randomly packed structure act as electron donors to Zr atoms, thus reducing ionization energy in the local clusters and causing a decrease in the interatomic distance and therefore a corresponding increase in density.

A self-evident inference from the above observations is that interatomic separations in amorphous metallic alloys are reduced compared to those found in their crystalline forms, thus giving densities that are higher than those expected from the geometrical hard sphere (same occupied volume) packing model predictions.

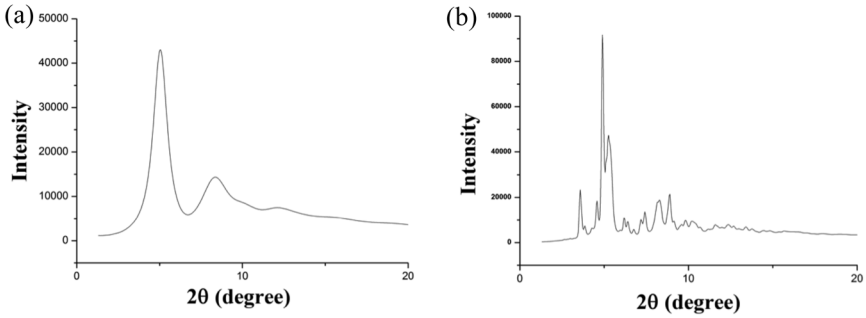

FIG. 6. X-ray diffraction intensities obtained from the $Zr_{64.13}Cu_{15.75}Ni_{10.12}Al_{10}$ alloy at room temperature. (a) For the as-cast amorphous glassy state. (b) For the semicrystalline state after annealing at 870 K. Synchrotron radiation, λ = 0.020 728 nm (GW—unpublished results).

The DFT computations described above for aluminum clusters corroborate this effect.

CONCLUSIONS

- Evidence against the proposition that existence of localized SRO/MRO domains is necessary for the closeness in the density of metallic glasses and their crystalline counterparts is presented. We acknowledge that such domains likely do exist in many glasses but our calculations demonstrate that they are not a prerequisite for the structure to achieve the correct density values. Moreover, we suggest that deviations from overall randomness may occur and that the overall average bond-lengths be preserved to yield the correct density. One must accept that the amorphous structure of real metallic glasses is based predominantly on random packing of atoms, with minimal presence of ordered clusters. Consequently, this hypothesis should be dismissed as invalid. Of course, this does not preclude the presence of ordered clusters in amorphous solids,[29,38,49] which should be described as faults (defects) within random packing.[59]
- DFT computations on aluminum clusters confirm the relaxation of the bonds with reduced coordination, and therefore, a reduction in the atomic Voronoi volume. It is conjectured that this effect accounts for the density of amorphous metals being so close to that of the corresponding crystalline forms. This evidence supports the RIS hypothesis.
- The density of covalent (saturated) amorphous solids is predicted adequately by the method of random packing of spheres. The bond lengths do not depend on the atomic arrangements since the electronic structure is tightly bound and not affected by coordination. The RIS hypothesis does not apply to these solids.
- There is no general rule for the density of amorphous solids with ionic bonds, other than the five Pauling rules on crystal structures. Each ionic system must be considered individually, as examples of positive and negative density variations occur (see Table I).

ACKNOWLEDGMENTS

The computational part of this research was undertaken with the assistance of resources from the National Computational Infrastructure (NCI), which is supported by the Australian Government under the National Collaborative Research Infrastructure Scheme (NCRIS) program.

APPENDIX: DETAILS OF DTF APPROACH TO fcc CLUSTER

For the 43-atom fcc cluster in Fig. 2, three different treatments were applied for atomic relaxation: (i) "Fully relaxed cluster" means in vacuum with the corresponding 1st d_{NN}, 2nd d_{NN}, and 3rd d_{NN} distances all changed from those of the bulk; (ii) "fix 2nd and 3rd clusters" means fixed 2nd and 3rd nearest neighbors as in bulk fcc (thus as 0.4040 nm and 0.4948 nm) and only relaxed the central 13 Al atoms, the corresponding 1st d_{NN} is now 0.2864 nm; (iii) "fix the 3rd cluster," only the 3rd d_{NN} atoms are fixed, and relaxed the 13 + 6 atoms; thus, both the 1st d_{NN} and 2nd d_{NN} distances change. The results are summarized in Table IV.

Focusing on the 1st d_{NN} values, one can see that case (ii) gives a better result than case (iii), but it is still a little far from the bulk. One can envisage that for a very big cluster model, if only the central part is relaxed, these d_{NN} values should converge to the bulk value.

Therefore, one can expect that the larger the size of the cluster, the more accurate results are obtained. Here, one has to balance the cost/efficiency and accuracy. For the amorphous clusters, we have used much larger clusters, 100 atoms, and only allowed the central +1st d_{NN} atoms to relax, as shown in Fig. 1.

REFERENCES

[1] A. Alam and D. D. Johnson, "Structural properties and relative stability of (meta)stable ordered, partially ordered, and disordered Al-Li alloy phases," Phys. Rev. B **85**, 144202 (2012).
[2] A. Alam and D. D. Johnson, "Mixed valency and site-preference chemistry for cerium and its compounds: A predictive density-functional theory study," Phys. Rev. B **89**, 235126 (2014).
[3] A. Alam, M. Khan, R. W. McCallum, and D. D. Johnson, "Site-preference and valency for rare-earth sites in $(R\text{-}Ce)_2Fe_{14}B$ magnets," Appl. Phys. Lett. **102**, 042402 (2013).
[4] C. Annic, J. Troadec, A. Gervois, J. Lemaitr, M. Ammi, and L. Oger, "Experimental study of radical tessellations of assemblies of discs with size distribution," J. Phys. I **4**(1), 115–125 (1994).
[5] M. J. Assael, K. Kakosimos, R. M. Banish, J. Brillo, I. Egry, R. Brooks, P. N. Quested, C. Mills, A. Nagashima, Y. Sato, and W. A. Wakeham, "Reference data for the density and viscosity of liquid aluminium and liquid iron," J. Phys. Chem. Ref. Data **35**(1), 285–290 (2006).
[6] S. Basak, R. Clarke, and S. R. Nagel, "Pair distribution function and its relation to the glass transition in an amorphous alloy," Phys. Rev. B **20**(8), 3388–3390 (1979).
[7] J. Blumm and J. B. Henderson, "Measurement of the volumetric expansion and bulk density of metals in the solid and molten regions," High Temp. - High Pressures **32**, 109–113 (2000).

[8]J. A. Cahill and A. D. Kirshenbaum, "The density of liquid copper from its melting point and an estimate of its critical constants," J. Phys. Chem. **66**, 1080–1082 (1962).
[9]M. Calin, M. Stoica, J. Eckert, A. R. Yavari, and L. Schultz, "Glass formation and crystallisation of CuTiZrNiX alloys," Mater. Sci. Eng.: A **392**, 169–178 (2005).
[10]Y. Cao, J. C. Zhu, Z. S. Nong, X. W. Yang, Y. Liu, and Z. H. Lai, "First principles studies of the structural, elastic, electronic and thermal properties of Ni_3-Nb," Comput. Mater. Sci. **77**, 208–213 (2013).
[11]G. S. Cargill III, "Dense random packing of hard spheres as a structural model for noncrystalline metallic solids," J. Appl. Phys. **41**, 2248–2250 (1970).
[12]A. Caron, R. Wunderlich, D. V. Louzguine, T. Egami, and H.-J. Fecht, "On the glass transition temperature and the elastic properties in Zr-based bulk metallic glasses," Philos. Mag. Lett. **91**(12), 751–756 (2011).
[13]Y. Q. Cheng and E. Ma, "Atomic level structure and structure-property relationship in metallic glasses," Prog. Mater. Sci. **56**, 379–473 (2011).
[14]J. Cieślak, J. Przewoźnik, and S. M. Dubiel, "Structural and electronic properties of the μ-phase Fe–Mo compounds," J. Alloys Compd. **612**, 465–470 (2014).
[15]X. Y. Cui and S. P. Ringer, "On the nexus between atom probe microscopy and density functional theory simulations," Mater. Charact. **146**, 347 (2018).
[16]X. Y. Cui, J. E. Medvedeva, B. Delley, A. J. Freeman, N. Newman, and C. Stampfl, "Role of embedded clustering in dilute magnetic semiconductors: Cr doped GaN," Phys. Rev. Lett. **95**, 256404 (2005).
[17]J. C. de Lima, A. R. Jeronimo, T. O. Almedia, T. A. Grandi, C. E. M. Campos, S. M. Souza, and D. M. Triches, "Modelling the atomic structure of an amorphous $Ni_{71}Nb_{29}$ alloy produced by mechanical alloying using reverse Monte Carlo simulations," J. Non-Cryst. Solids **353**, 1046–1053 (2007).
[18]B. Delley, "An all-electron numerical method for solving the local density functional for polyatomic molecules," J. Chem. Phys. **92**(1), 508–517 (1990).
[19]B. Delley, "From molecules to solids with the $DMol^3$ approach," J. Chem. Phys. **113**(18), 7756–7764 (2000).
[20]I. Douglass, T. Hudson, and P. Harrowell, "Density and glass forming ability in amorphous atomic alloys: The role of the particle softness," J. Chem. Phys. **144**, 144502 (2016).
[21]T. Egami, S. J. Poon, Z. Zhang, and V. Keppens, "Glass transition in metallic glasses: A microscopic model of topological fluctuations in the bonding network," Phys. Rev. B **76**, 024203-1–024203-6 (2007).
[22]S. R. Elliott, "Origin of the first sharp diffraction peak in the structure factor of covalent glasses," Phys. Rev. Lett. **67**(6), 711–714 (1991).
[23]T. Fang, S. J. Kennedy, L. Quan, and T. J. Hicks, "The structure and paramagnetism of Ni_3Nb," J. Phys.: Condens. Matter **4**, 2405–2414 (1992).
[24]R. X. Feng, Z. H. Stachurski, M. D. Rodriguez, P. Kluth, L. L. Araujo, and M. C. Ridgway, "X-ray scattering from amorphous solids," J. Non-Cryst. Solids **383**, 21–27 (2014).
[25]P. J. Flory, *Principles of Polymer Chemistry* (Cornell University Press, Ithaca, NY, USA, 1967).
[26]F. C. Frank and J. S. Kasper, "Complex alloy structures regarded as sphere packings. I. Definitions and basic principles," Acta Crystallogr. **11**(3), 184–190 (1958).
[27]G. Gutierrez and B. Johansson, "Molecular dynamics study of structural properties of amorphous Al_2O_3," Phys. Rev. B **65**, 104202 (2002).
[28]A. Hirata, P. Guan, T. Fujita, Y. Hirotsu, A. Inoue, A. R. Yavari, T. Sakurai, and M. Chen, "Direct observation of local atomic order in a metallic glass," Nat. Mater. **10**, 28–33 (2011).
[29]T. C. Hufnagel, "Amorphous materials: Finding order in disorder," Nat. Mater. **3**, 666–667 (2004).
[30]A. Inoue and A. Takeuchi, "Recent progress in bulk glassy alloys," Mater. Trans. **43**, 1892–1906 (2002).
[31]L. N. Kolotova, G. E. Norman, and V. V. Pisarev, "Glass transition of aluminium melt: Molecular dynamics study," J. Non-Cryst. Solids **429**, 98–103 (2015).
[32]M. Krbal, A. V. Kolobov, B. Hoyt, B. Andre, P. Fons, R. E. Simpson, T. Uruga, H. Tanida, and J. Tominaga, "Amorphous InSb: longer bonds yet higher density," J. Appl. Phys. **108**, 023506–023515 (2010).
[33]P. F. Lang and B. C. Smith, "Ionic radii for group 1 and group 2 halide, hydride, fluoride, oxide, sulfide, selenide and telluride crystals," Dalton Trans. **39**(33), 7786–7791 (2010).
[34]M. Laso, N. C. Karayiannis, K. Foteinopoulou, M. L. Mansfield, and M. Kroger, "Random packing of model polymers: Local structure, topological hindrance and universal scaling," Soft Matter **5**, 1762–1770 (2009).
[35]J. C. Lee, K. W. Park, K. H. Kim, E. Fleury, B. J. Lee, M. Wakeda, and Y. Shibutani, "Origin of the plasticity in bulk amorphous alloys," J. Mater. Res. **22**(11), 3087–3097 (2007).
[36]M. Leitner, T. Leitner, A. Schmon, K. Aziz, and G. Pottlacher, "Thermophysical properties of liquid aluminium," Metall. Mater. Trans. A **48**, 3036–3045 (2017).
[37]Y. Li, Q. Guo, J. A. Kalb, and C. V. Thompson, "Matching glass-forming ability with the density of the amorphous phase," Science **322**(5909), 1816–1819 (2008).
[38]E. Ma, "Tuning order in disorder," Nat. Mater. **14**, 547–552 (2015).
[39]I. Martin, T. Ohkubo, M. Ohnuma, B. Deconihout, and K. Hono, "Nanocrystallisation of $Zr_{41.2}Cu_{12.5}Ni_{10}Ti_{13.8}Be_{22.5}$ metallic glass," Acta Mater. **52**, 4427 (2004).
[40]D. B. Miracle, "A structural model for metallic glasses," Nat. Mater. **3**(10), 697–702 (2004).
[41]M. Muller, J. Nievergelt, S. Santos, and U. W. Suter, "A novel geometric embedding algorithm for efficiently generating dense polymer structures," J. Chem. Phys. **114**(22), 9764–9771 (2001).
[42]P. Nash and A. Nash, "The Nb-Ni system," Bull. Alloy Phase Diagrams **7**(2), 124–129 (1986).
[43]B. Noble, S. J. Harris, and K. Dinsdale, "The elastic modulus of aluminium-lithium alloys," J. Mater. Sci. **17**(2), 461–468 (1982).
[44]K. W. Park, J. I. Jang, M. Wakeda, Y. Shibutani, and J. C. Lee, "Atomic packing density and its influence on the properties of Cu-Zr amorphous alloys," Scr. Mater. **57**, 805–808 (2007).
[45]J. P. Perdew, K. Burke, and M. Ernzerhof, "Generalized gradient approximation made simple," Phys. Rev. Lett. **77**(18), 3865–3868 (1996).
[46]D. E. Polk, "The structure of glassy metallic alloys," Acta Metall. **20**, 485–491 (1972).
[47]R. G. Quynn, J. L. Riley, D. A. Young, and H. D. Noether, "Density, crystallinity, and heptane insolubility in isotactic polypropylene," J. Appl. Polym. Sci. **2**(5), 166–173 (1959).
[48]P. S. Salmon, "Real space manifestation of the first sharp diffraction peak in the structure factor of liquid and glassy materials," Proc. R. Soc. London, Ser. A **445**, 351–365 (1994).
[49]P. S. Salmon, "Amorphous materials: Order within disorder," Nat. Mater. **1**(2), 87–88 (2002).
[50]C. Shi, O. L. G. Alderman, D. Berman, J. C. Du, J. Neuefeind, A. Tamalonis, J. K. Weber, J. G. You, and C. J. Benmore, "The structure of amorphous and deeply supercooled liquid alumina," Front. Mater. **6**, 1–15 (2019).
[51]R. K. Singh, S. Y. Wu, H. X. Liu, L. Gu, D. J. Smith, and N. Newman, "The role of Cr substitution on the ferromagnetic properties of $Ga_{1-x}Cr_xN$," Appl. Phys. Lett. **86**(1), 012504 (2005).
[52]Z. H. Stachurski, "Yield strength and anelastic limit of amorphous ductile polymers," J. Mater. Sci. **21**, 3231–3236 (1986).
[53]Z. H. Stachurski, "Definition and properties of ideal amorphous solids," Phys. Rev. Lett. **90**(15), 5502 (2003).
[54]Z. H. Stachurski, "On structure and properties of amorphous materials," Materials **4**, 1564–1598 (2011).
[55]H. W. Starkweather and R. E. Moynihan, "Density, infrared absorption, and crystallinity in 66 and 610 nylons," J. Polym. Sci. **22**, 363–368 (1956).
[56]Y. L. Sun and J. Shen, "Icosahedral ordering in $Cu_{60}Zr_{40}$ metallic glass: Molecular dynamics simulations," J. Non-Cryst. Solids **355**(31-33), 1557–1560 (2009).
[57]E. Svab, F. Forgacs, F. Hajdu, N. Kroo, and J. Takacs, "Partial correlations in $Ni_{60}Nb_{40}$ metallic glass," J. Non-Cryst. Solids **46**, 125–134 (1981).
[58]D. N. Theodorou and U. W. Suter, "Atomistic modelling of mechanical properties of polymeric glasses," Macromolecules **19**, 139–154 (1986).

[59]L. Th. To, D. J. Daley, and Z. H. Stachurski, "On the definition of an ideal amorphous solid of uniform hard spheres," Solid State Sci. **8**, 868–879 (2006).
[60]X. Tong, G. Wang, Z. H. Stachurski, B. Bednarcik, N. Mattern, Q. J. Zhai, and J. Eckert, "Structural evolution and strength change of a metallic glass at different temperatures," Sci. Rep. **6**, 30876 (2016).
[61]M. M. J. Treacy and K. B. Borisenko, "The local structure of amorphous silicon," Science **335**, 950–953 (2012).
[62]M. Wakeda, Y. Shibutani, Sh. Ogata, and J. Y. Park, "Relationship between local geometrical factors and mechanical properties for Cu-Zr amorphous alloys," Intermetallics **15**, 139–144 (2007).
[63]N. Wanderka, M.-P. Macht, M. Seidel, and S. Mechler, "Formation of quasicrystals in ZrTiCuNiBe bulk glass," Appl. Phys. Lett. **77**(24), 3935–3937 (2000).
[64]G. Wang, J. Shen, J. F. Sun, B. D. Zhou, J. D. FitzGerald, D. Llewellyn, and Z. H. Stachurski, "Isothermal nanocrystallisation behavior of ZrTiCuNiBe bulk metallic glass in the supercooled region," Scr. Mater. **53**, 641–645 (2005).
[65]W. H. Wang, "The elastic properties, elastic models and elastic perspectives of metallic glasses," Prog. Mater. Sci. **57**(3), 487–656 (2012).
[66]R. W. G. Wyckoff, *The Structure of Crystals*, 2nd ed. (Reinhold Publishing Corporation, New York, USA, 1935).
[67]J. Zarzycki, *Glasses and the Vitreous State* (Cambridge University Press, Cambridge, 1991).
[68]A. V. Zhalko-Titarenko, M. L. Yevlashina, V. N. Antonov, B. Yu. Yavorskii, Yu. N. Koval, and G. S. Firstov, "Electronic and crystal structure of the ZrCu intermetallic compound close to the point of structural transformation," Phys. Status Solidi B **184**, 121–128 (1994).
[69]L. N. Zou, X. Cheng, M. L. Rivers, H. M. Jaeger, and S. R. Nagel, "The packing of granular polymer chains," Science **326**(5951), 408–410 (2009).